

Wideband air – coupled ultrasonic transducers

R. Kažys, A. Vladišauskas, E. Žukauskas

Prof. K. Baršauskas ultrasound institute

Kaunas University of Technology

Introduction

There are many applications of air – coupled ultrasonics in nondestructive evaluation [1], distance [2] and thickness measurements [3], testing of diffusion bonds [4], investigation of surfaces of the objects [5], flow measurements [6] and etc. The air – coupled ultrasonic investigation of materials is very attractive, because it avoids the disadvantages caused by liquid or semi - liquid couplants, especially in cases when humidity can change properties of the materials or even destroy the material, such as honeycomb structure. Also use of contact ultrasonic systems is restricted in the case of complex geometry structures. The most common air – coupled ultrasonic transducers are based on piezoelectric and electrostatic effects. The transducers of the first type exploit piezoelectric materials such as PZT, and tend to be resonant, and therefore require a special backing in order to obtain good damping. However, they can be used in the industrial applications where robust construction is important [7], including the flow meters of high pressure gases [8,9]. The mismatch of the specific acoustic impedances between most piezoelectric materials and gasses can be improved using the matching layers. Also application of the matching layers improves bandwidth of the piezoelectric transducers.

Objective of this work was to develop robust wideband air – coupled ultrasonic transducers, suitable for industrial applications and to investigate their.

Design of the transducer

The schematic drawing of the air – coupled ultrasonic transducer is shown in Fig.1. The wideband and sensitive ultrasonic transducer is developed using the matching layers. The front face matching was achieved using two quarter – wave layers 1, 2. The back face of the piezoelement 3 is loaded with one quarter – wave matching layer 4. All this construction (front matching layers, piezoelement, the back matching layer) is glued together and fixed by a metallic ring 5. the inner diameter of the metallic ring 5 is bigger than the diameter of the piezoelement 3 and filled with a high – loss backing material 6. The front side of the first matching layer is glued to the housing of the transducer. All inner space of the transducer is filled with a high – loss backing material such as a tungsten – epoxy mixture. This rigid construction provides service ability under a high pressure and long time operation of the transducer.

To improve sensitivity of the ultrasonic transducers the air backed piezoelectric elements can be used. Using resonant systems only one transducer can give increase in

sensitivity nearly 10 times (20 dB) compared to conventional damped transducers, but such a design is fragile. Moreover, the ultrasonic transducers with an air backing are narrowband.

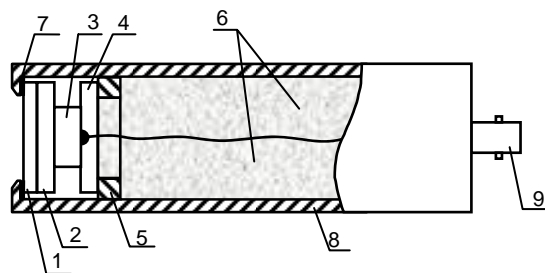


Fig. 1. Schematic drawing of the air – coupled transducer structure: 1, 2 – front face matching layers; 3 – piezoelement of the transducer; 4 – back matching layer; 5 – metallic ring; 6 – high – loss back material; 7 – glue; 8 – housing of the transducer; 9 – connector

Modeling of transfer functions of the ultrasonic transducer

Graphical representation of the model of the multilayered air – coupled ultrasonic transducer is shown in Fig. 2.

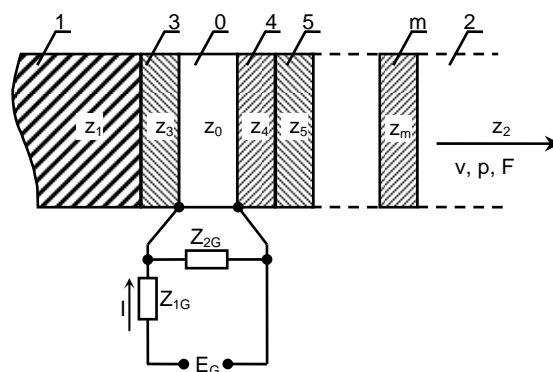


Fig. 2. Model of ultrasonic transducer. 0 – piezoelement, 1 - damper, 2 – surrounding media, 3 – back matching layer, 4, 5...m – front matching layers, E_G – electric voltage, I – current, Z_{1G} , Z_{2G} – electrical impedances

The transfer function of such a multilayered structure can be obtained using one – dimensional approach based on a matrix calculus. The matrix equation of the multilayered structure can be written as [11], [12]:

$$\begin{bmatrix} E_G \\ I \end{bmatrix} = [A^*] \cdot \begin{bmatrix} F \\ v \end{bmatrix}, \quad (1)$$

where $[A^*]$ is the matrix of the transducer, F and v are the force and the particle velocity on the boundary between the m -th matching layer and the surrounding media. The matrix of the ultrasonic transducer $[A^*]$ is described by the following equation:

$$[A^*] = \begin{bmatrix} 1 & Z_{1G} \\ 0 & 1 \end{bmatrix} \cdot \begin{bmatrix} \frac{1}{Z_{2G}} & 0 \\ \frac{1}{Z_{2G}} & 1 \end{bmatrix} \cdot [A] \cdot [S^{(m)}], \quad (2)$$

where $[A]$ is the matrix of the piezoelement, $[S^{(m)}]$ is the matrix of the system of the front matching layers. The matrix for one non piezoelectric layer can be written as:

$$[S^{(i)}] = \begin{bmatrix} \cosh \gamma_i d_i & \frac{\sinh \gamma_i d_i}{Z_i} \\ Z_i \sinh \gamma_i d_i & \cosh \gamma_i d_i \end{bmatrix}, \quad (3)$$

where $\gamma_i = \alpha_i(\omega) + j2\pi/\lambda_i$, $\alpha_i(\omega)$ is the attenuation coefficient of an ultrasonic wave in the i -th layer, $\lambda_i = c_i/f$ is the wavelength of an ultrasonic wave in the i -th layer, c_i is the phase velocity of an ultrasonic wave in the i -th layer, d_i is the thickness of the i -th layer, Z_i is the acoustic impedance of the i -th layer, $\omega = 2\pi f$, $j = \sqrt{-1}$. The matrix of a multilayered structure can be obtained multiplying in consecutive order the individual matrixes of all layers.

The transfer function of the multilayered piezotransducer can be calculated from the transducer matrix coefficients using the following equation:

$$K(f) = \frac{1}{A_{11}^* + \frac{A_{12}}{z_2}}. \quad (4)$$

Calculations were carried out for several cases. The transfer function for a damped (tungsten – epoxy mixture $z_1=6.2$ Mrayl) piezoelement without matching layers, the transfer function of the transducer with one front quarter wave matching layer (fiberglass $z_4 = 4.48$ Mrayl), the transfer function of the transducer with two front quarter wave matching layers (fiberglass $z_4 = 4.48$ Mrayl and silicone $z_5 = 1.12$ Mrayl), the transfer function with two quarter wave front matching layers and one quarter wave back matching layer (fiberglass $z_3 = 4.48$ Mrayl) were calculated. The influence of an electrical matching circuit was evaluated as well. Electrical matching circuit consists of inductance ($Z_{1G} = j\omega L$) and resistance ($Z_{2G} = R$).

Results of calculations are presented in Fig. 3 and Fig.4. It is essential to notice, that all curves are normalized according to the curve 1 in Fig. 3 and Fig. 4. Fig.3 and Fig.4 show that ultrasonic transducers without matching layers have only one maximum at the resonant frequency. Application of one quarter wave fiberglass matching layer increases the transfer function value more than 5dB and allows to widen the bandwidth (Fig. 3, curve 2). Higher efficiency and wider bandwidth can be achieved adding on two quarter wave front matching layers which are made of fiberglass and silicone. In this case the transmission coefficient increases by 12 dB (Fig. 3, curve 3).

Application of the back quarter wave matching layer allows increase the transmission coefficient up to 17 dB (Fig. 4, curve 2). Peaks of the transfer function can be

flattened and efficiency increased using electrical matching circuits.

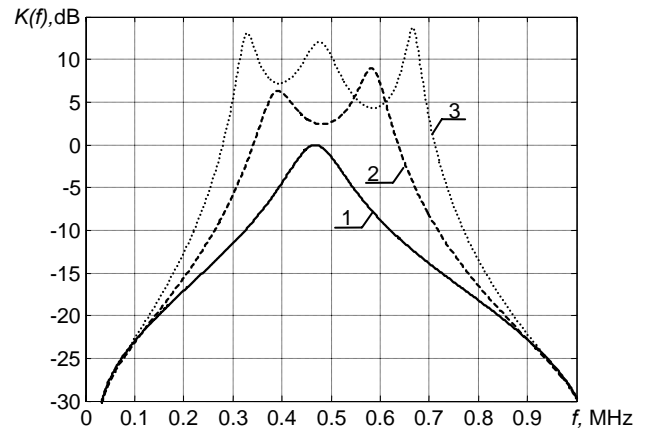


Fig. 3. Calculated transfer functions of the air – coupled ultrasonic transducer. 1 – transfer function of damped transducer without matching layers, 2 – transfer function of damped transducer with single $\lambda/4$ front matching layer, 3 - transfer function of damped transducer with double $\lambda/4$ front matching layer

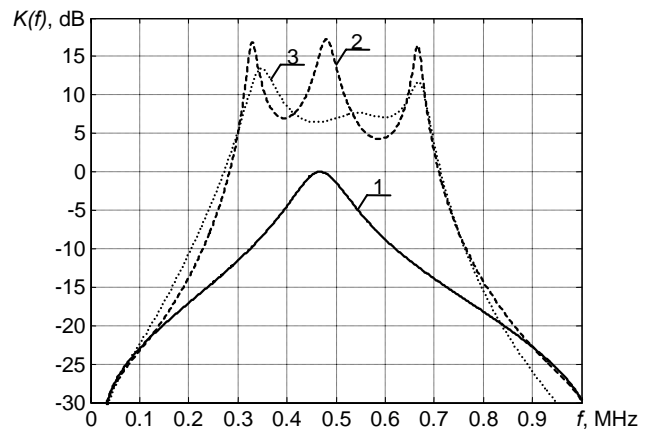


Fig. 4. Calculated transfer functions of the air – coupled ultrasonic transducer. 1 – transfer function of damped transducer without matching layers, 2 – transfer function of damped transducer with double $\lambda/4$ front and single $\lambda/4$ back matching layers, 3 - transfer function of damped transducer with double $\lambda/4$ and single $\lambda/4$ back matching layers and electrical matching circuit.

Experimental setup

The block diagram of the experimental system is shown in Fig.5.

All components of this system can be divided into three main parts: the transmitter unit, the receiver unit and the scanner.

The transmitter part consists of the low voltage arbitrary waveform Hewlett Packard HP33120A generator and the high voltage generator. Maximal voltage at the output of the high voltage generator is 500V. Voltage can be increase up to 2500V using transformers. For excitation of the transmitter sine burst signals were used.

The receiver part is composed of the following elements: preamplifier and amplifier with a gain control. The low noise 40dB preamplifier is connected directly to the receiver in order to improve signal to noise ratio. The

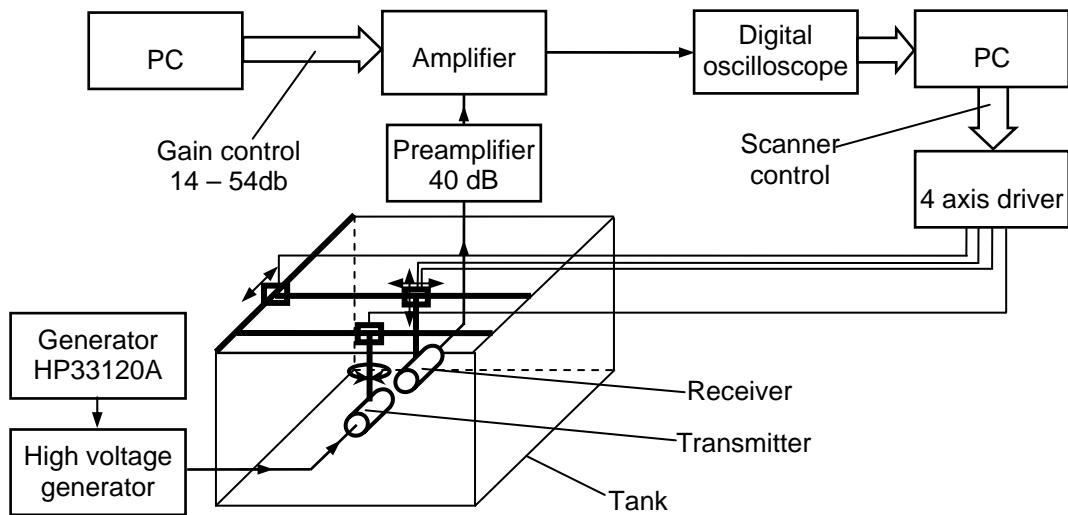


Fig.5. Block diagram of the experimental system

main amplifier is controlled by a personal computer via PC104 bus. Gain of the amplifier can be changed from 14dB to 54dB. Bandwidth of the amplifier is from 200 kHz to 1 MHz.

The signals at the output of the amplifier are captured by the Hewlett Packard HP54645A digital oscilloscope. If signal to noise ratio is very low, the signals can be averaged by the oscilloscope. Averaging of the signals can give significant improvement of the signal to noise ratio, but measuring time can dramatically increase depending on an averaging number. After that signals are transferred via the IEEE – 488 interface to a PC for storage and processing. The scanning system is designed in such a way that the ultrasonic transmitter is at the fixed position and the ultrasonic receiver is moved during the scanning process.

Experimental investigation of air – coupled ultrasonic transducers

Experimental investigations of the air – coupled ultrasonic transducers were performed using the 500 kHz piezotransducer at the different distances – from 50 mm to 500 mm. Duration of the excitation pulses were from half to eight periods.

The excitation pulse of the half period is presented in Fig. 6. Duration of the pulse is 1 μ s and amplitude of the pulse is 4.7 V. The spectrum of this pulse is shown in Fig. 7. The width of the spectrum at the -6 dB level is 750 kHz. The received and amplified ultrasonic signal after excitation with the half period pulse is shown in Fig. 8. In this case the distance between transducers was 50 mm. The spectrum of this signal is shown in Fig. 9 (curve 1). The width of the signal spectrum at the -6 dB level is 250 kHz and what corresponds to 48% from the central frequency of the transducer. When the distance between transducers increases, the amplitudes of spectrum decreases (Fig. 9). Also the width of the signal spectrum becomes narrow due to the frequency dependent attenuation in air. The spectrum of the signal depends on the spectrum of the excitation signal as well. The main part of the spectrum of

the received signal covers spectrum of the excitation signal between points A and B (Fig. 7.). Decrease of the amplitude of the spectrum of the excitation pulse agree with the spectrum of the received signal (points C and D in Fig. 9) only at small distances between transducers, when attenuation of ultrasonic waves in air can be neglected. For bigger distances this does not hold.

The improvement of the amplitude of the received signal and his spectrum can be obtained using an excitation pulse with the symmetrical spectrum. An example of two periods excitation pulse and his spectrum are shown in Fig. 10 and Fig. 11. The maximum of spectrum is a little bit displaced from the transducers central frequency. The signal at the output of the amplifier, when distance between transducers is 50 mm, is shown in Fig. 12. Dependence of the spectrum of the received signals on distances from 50 mm to 300 mm is shown in Fig. 13. In this case the components of spectrum are changed. The amplitude of frequency 550 kHz at the point H is higher than the amplitude at the point G. It gives two maximums in the spectrum of the received signals (points E and F). These points corresponds to the points H and G in spectrum of the excitation signal. At the 100 mm distance between transducers both amplitude maximums are equal. In this way spectrum of the wideband air – coupled ultrasonic transducers can be adjusted by excitation pulse at different distances. Example of the narrowband 8 periods excitation pulse and its spectrum is shown in Fig.14 and Fig. 15. A long excitation pulse (Fig. 14) gives more concentration of the spectrum components about 500kHz within a narrow band (Fig. 15). The maximum of the spectrum precisely corresponds to the central frequency of the transducers. The signal at the output of the amplifier when distance between transducers is 50 mm is shown in Fig. 16. Dependence of the spectrum of the received signals on distances from 50 mm to 300 mm is shown in Fig. 17. Using narrowband signals for excitation of the wideband transducers allows tuning frequency of the ultrasonic wave for specific tasks. The experimentally measured transfer functions are shown in Fig. 18.

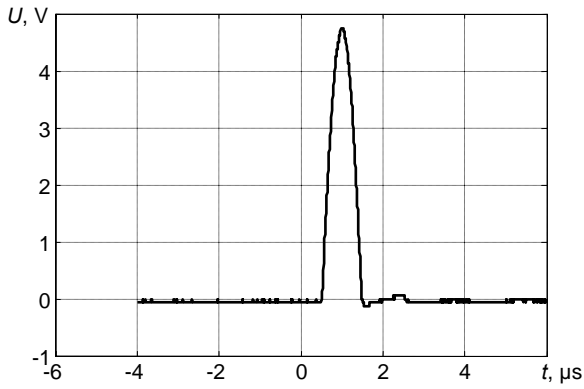


Fig.6. Time diagram of 0.5 period excitation signal

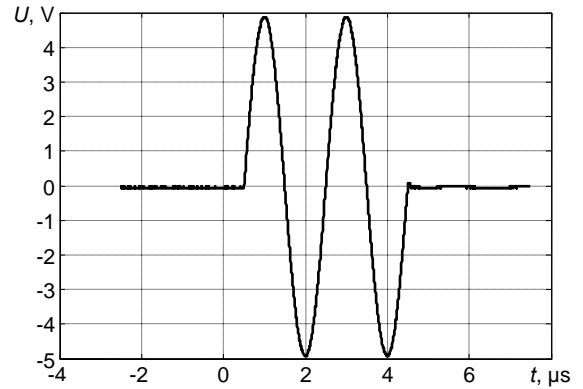


Fig.10. Time diagram of 2 periods excitation signal

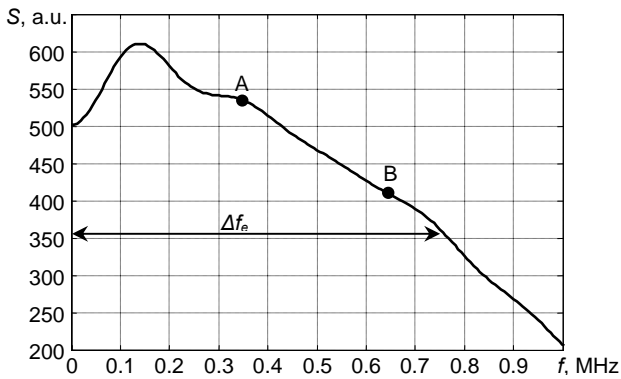


Fig.7. Spectrum of excitation signal; a.u. – arbitrary units

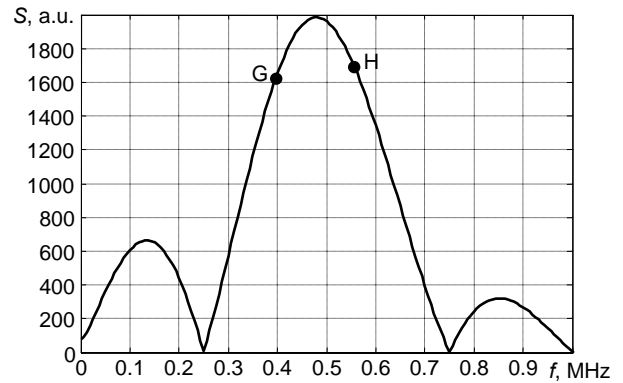


Fig.11. Spectrum of excitation signal; a.u. – arbitrary units

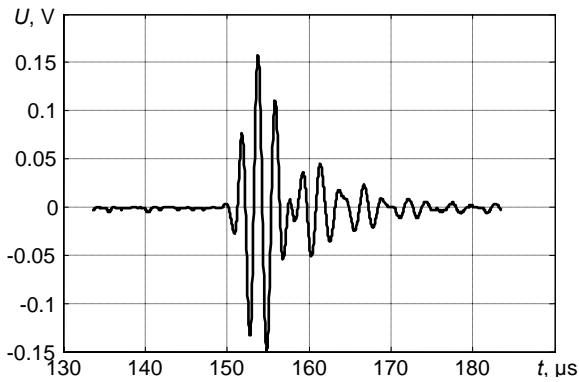


Fig.8. Signal on an output of the amplifier when distance between transducers 50mm. Duration of excitation signal – 0.5 period.

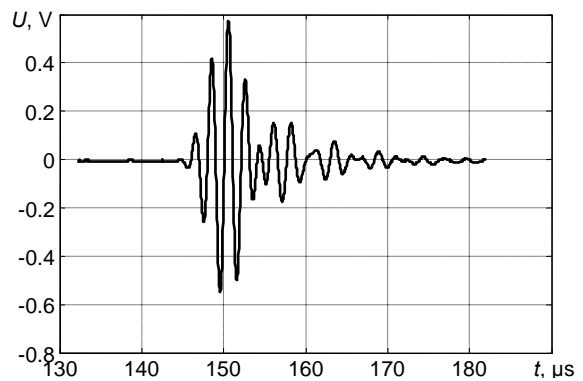


Fig.12. Signal on an output of the amplifier when distance between transducers 50mm

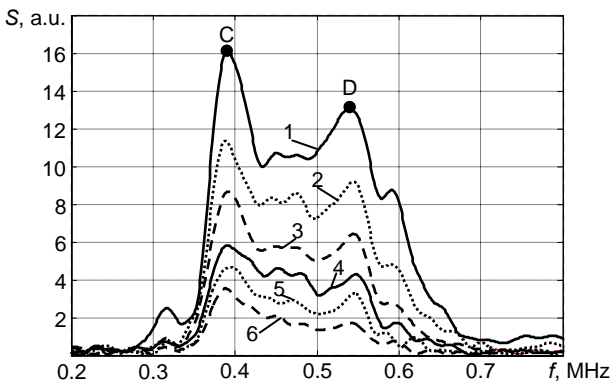


Fig.9. Dependence of a spectrum of the signal vs. distance between transducers. Distances between transducers: 1- 50mm, 2 – 100mm, 3 – 150mm, 4 – 200mm, 5 – 250mm, 6 – 300mm.

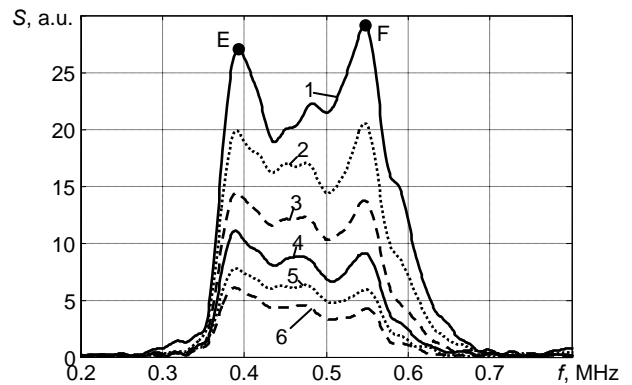


Fig.13. Dependence of a spectrum of the signal vs. distance between transducers. Distances between transducers: 1- 50mm, 2 – 100mm, 3 – 150mm, 4 – 200mm, 5 – 250mm, 6 – 300mm.

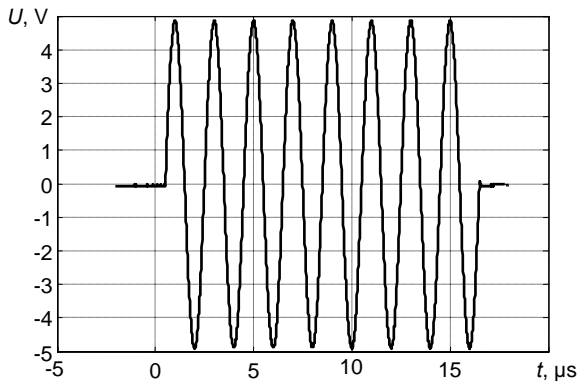


Fig.14. Time diagram of 8 periods excitation signal

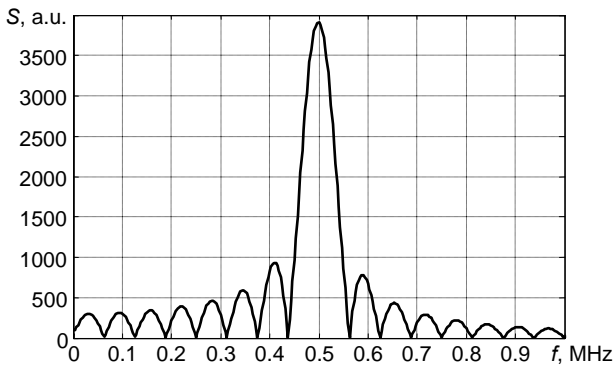


Fig.15. Spectrum of excitation signal; a.u. – arbitrary units

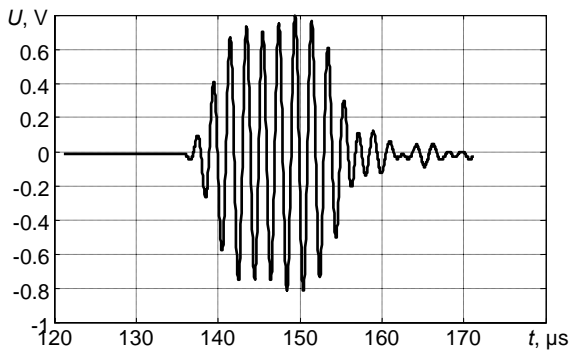


Fig.16. Signal at the output of the amplifier when the distance between transducers 50 mm.

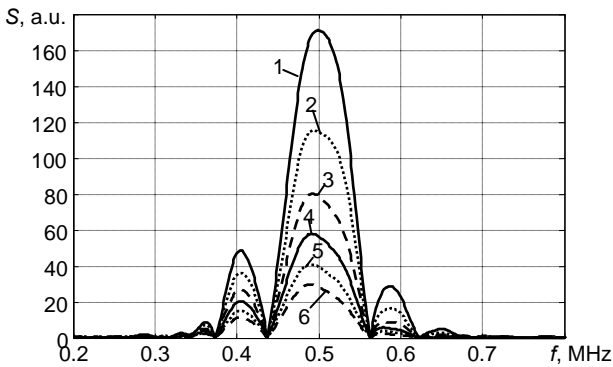


Fig.17. Dependence of a spectrum of the signal vs. distance between transducers. Distances between transducers: 1- 50mm, 2 – 100mm, 3 – 150mm, 4 – 200mm, 5 – 250mm, 6 – 300mm.

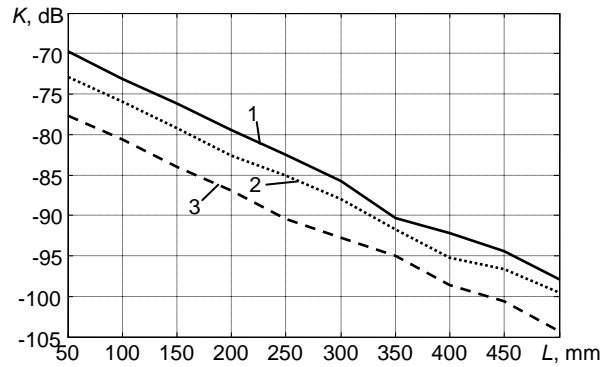


Fig.18. Transmission losses of air – coupled ultrasonic transducers vs. distance between the transducers when duration of the excitation pulse is 1 – 8 periods, 2 – 2 periods, 3 – 0.5 periods.

Experimental investigation of aerospace materials

Investigation of aerospace materials is one of the most important NDT tasks. Generally in most cases testing is performed using various couplants. However, in many non – destructive evaluation tasks, such as investigation of aerospace composite, honeycomb structures, whose properties may be changed or destroyed by liquid or semi liquid couplants, this technique can not be used. Also, liquid coupling can not be used when water can fill defects and the detectability of the defects may be reduced. In the mentioned cases air – coupled ultrasonic investigation of materials is very attractive, because it avoids the disadvantages caused by liquid or semi liquid couplants. However, there are some problems associated with air-coupled ultrasonic technique. The first of all, significant mismatch of acoustical impedances between ultrasonic transmitter/receiver, air and the material under the test. At a single interface between water ($Z=1.5 \text{ MRayl}$) and carbon fiber reinforced plastic ($Z=4.5 \text{ MRayl}$) the transmission coefficient is 0.75, but at interface between air ($Z=0.0004 \text{ MRayl}$) and carbon fiber reinforced plastic the transmission coefficient is only $3.55 \cdot 10^{-4}$. So, when the coupling medium is air, the energy transmission coefficient is very small. The second problem, but not so important like the previous, is attenuation of ultrasonic energy in air. Objectives of the following experiments were to verify possibility to investigate aerospace materials using wideband air – coupled ultrasonic transducers.

Experimental investigations of materials were carried out with two types of materials – glass fiber reinforced aluminum (GLARE3 – 3/2) and carbon fiber reinforced plastic (CFRP). These materials are in use in aerospace industry. The GLARE3 – 3/2 material is made of alternating layers of aluminum and fiberglass bonded together. The 1.4mm GLARE-3/2 plate was selected as a test sample. This sample consists of three layers 0.3mm aluminum alloy and two layers of 0.25mm thickness prepreg between aluminum. The prepreg layer is composed of two layers of glass fiber in an epoxy resin. Each prepreg layer is 0.125mm thick.

This test sample contains artificial delamination defects of the different diameters: 25, 12, 8, 6 and 3 millimeters. The defects are made of sealed teflon.

Experiments were carried out using two testing techniques – common through transmission testing technique and through transmission testing technique with Lamb waves. As the external layers of this material are made of aluminum, which is a high impedance material ($Z = 17\text{Mrayl}$), losses are more than 130 dB and signal to noise ratio is very low. Investigation of this test sample was carried out using signal averaging.

Fig.19 shows the amplitude C – scan of the GLARE3 – 3/2 samples with 25mm delamination defect. The experiment was carried out in the through transmission mode. The region of the delamination can be easily distinguished. Amplitudes of the transmitted ultrasonic signals are significantly different for both – defect free and defective zones. This difference can be clearly seen in a B – scan of the defective zone (Fig.20).

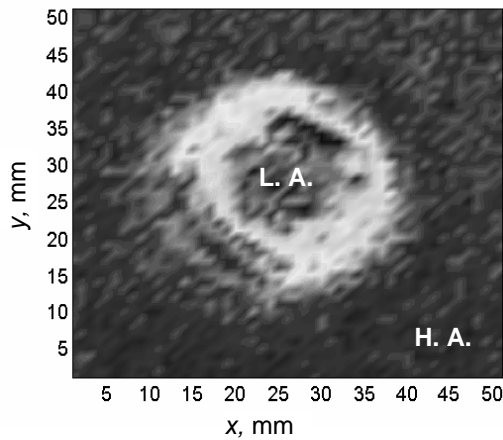


Fig.19. C - scan of the area with 25 mm defect carried out in the through transmission mode. (L.A. – low amplitude zone, H.A. – high amplitude zone)

Fig.21 shows the amplitude C – scan of the $50 \times 50\text{mm}^2$ area of the GLARE3 – 3/2 samples with 25mm delamination defect. Experiment was carried out using the through – transmission testing technique with the Lamb wave. Most important is that using Lamb waves the signal to noise ratio is better and the number of required averaged signals can be smaller, than in the through transmission testing technique. Fig.22 shows peak – to – peak amplitudes in the defect free and defective zones.

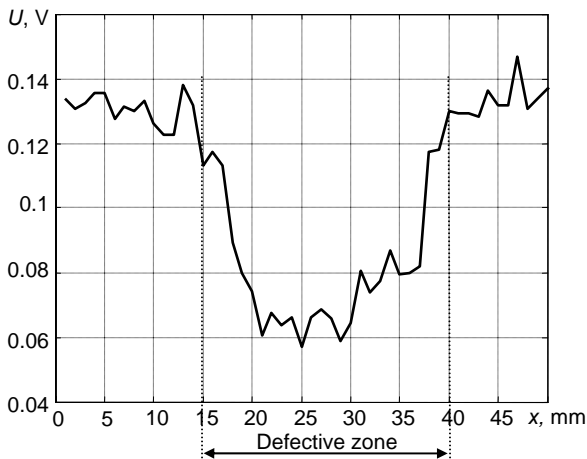


Fig.20. B – scan of the defective zone using through transmission testing technique

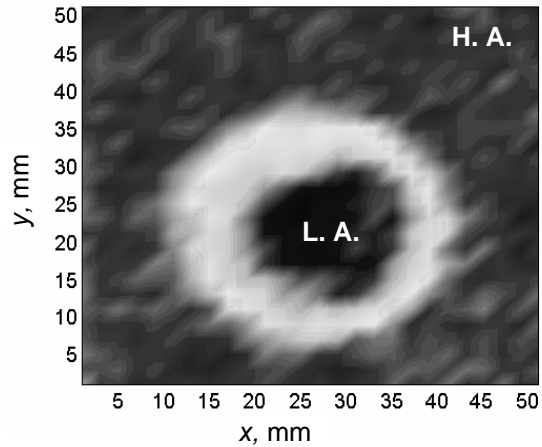


Fig.21. C - scan of the area with 25 mm defect carried out in the through transmission mode using a_0 Lamb wave. (L.A. – low amplitude zone, H.A. – high amplitude zone)

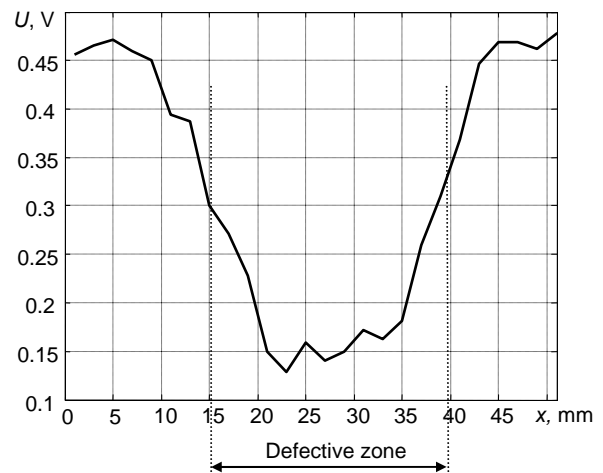


Fig.22. B – scan of the defective zone using through transmission testing technique with Lamb waves

Fig.20 and Fig.22 shows that using Lamb waves due to better impedance matching amplitudes of the signals are 3.2 times higher in the defect free zone and 2.5 times higher in the defective zone. Also ratio of the signals in the defect free and the defective zones is higher using Lamb waves.

The CFRP test samples were investigated using one – side testing technique with Lamb waves. These test samples contains impact damages of different intensity. Thickness of the sample is was not the same along the test sample (Fig.23), and testing by Lamb waves was complicated.

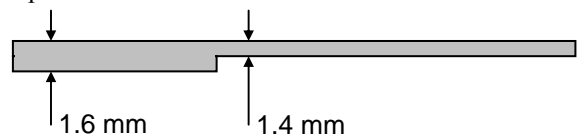


Fig. 23. Cross – section of the test sample

As the CFRP is a material of a low acoustic impedance, signal to noise ratio is significantly higher in comparison with high impedance materials (e.g. GLARE). One – side access experiments with Lamb waves were carried out without averaging of the signals.

Fig.24 shows the ultrasonic image of the CFRP plate with the 1J impact damage. The defect is very small and can not be detected visually. The dimensions of the investigated zone were 100×50 mm. The image of the impact defect looks elongated, because ultrasonic transducers are remote one from another. It is also possible to see variation in the thickness of the test sample as well.

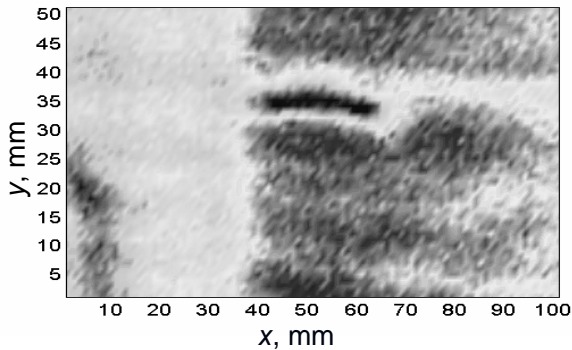


Fig. 24. The amplitude C – scan in one – side access mode with a_0 Lamb wave of the samples with impact defects: (a) – 1J impact defect,

Measurement of gas flow using air – coupled ultrasonic transducers

Objective of these experiments was to verify possibility to use wideband air – coupled transducers for measurement velocity of the gas flows up to 12m/s. The pressure of gases was up to 20 atmospheres.

Measurement of a gas flow velocity is based on measurement of the propagation time of ultrasonic signals. The main problems of are high attenuation of ultrasound in gases, strong fluctuations of the received signals due to turbulence and shift of the ultrasonic beam from the radiation direction caused by the high velocity flows. Due to these reasons the shape of the received ultrasonic signal is strong distorted, especially at high flow velocities. Measurements results can be improved using signal processing techniques. One of them is application coded sequences.

As coded sequences the Barker codes were used, which consisted of 11 or 13 elements. The Barker code was used for a phase modulation of the high frequency carrier. The frequency of the carrier was 500 kHz, which corresponds to the central frequency of the described air – coupled transducer.

The developed transducers were tested in air flows. Objective of the experiment was to determine how the transducers generate and receive wideband Barker codes, necessary for robust gas flow measurements. The measurements were performed in the measuring section with the 82 mm diameter at different flow velocities. The results of measurements are presented in Fig. 25 and Fig.26.

Even at the highest flow velocity $v = 8.5$ m/s the code is transmitted and received without essential distortions. The measurement error was up to 1.8% in all velocity range.

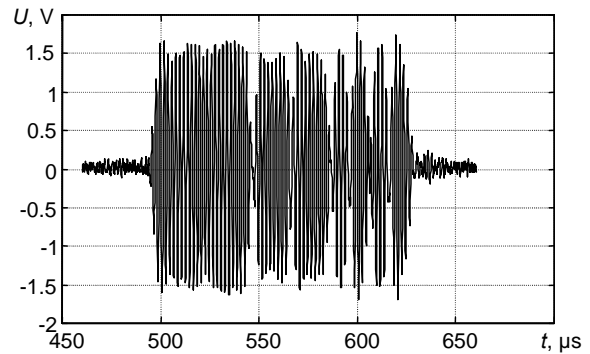


Fig.25. Received ultrasonic signal when the flow velocity 4.5m/s

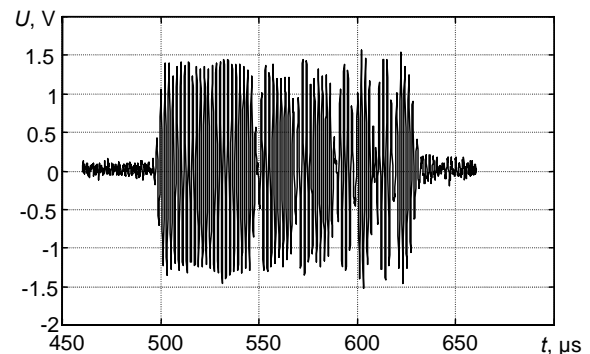


Fig.26. Received ultrasonic signal when the flow velocity 8.5m/s

Conclusions

The developed air – coupled ultrasonic transducers due to their design and optimal choice of the matching layers are suitable for many NDE and ultrasonic measurements tasks. Due to a wide bandwidth of the transducers it is possible to tune up the frequency of the excitation signal for specific cases independent of surrounding media. Due to a short transient response free these transducers are for excitation and reception of the coded sequences. The rigid construction of the transducers allows to use them in a high – pressure environment.

References

1. **Blome E., Bulcaen D., Declercq F.** Air – coupled ultrasonic NDE experiments in the frequency range 750kHz – 2MHz. *NDT&E International*. 2002. Vol.35. P. 417 – 426.
2. **Hickling R., Marin S.P.** The use of ultrasonics for gauging and proximity sensing in air. *J. Acoust. Soc. Am.* 1986. Vol.79. No.4. P.1151 – 1160.
3. **Schindel D. W., Hutchins D. A.** Through – thickness characterization of solids by wideband air – coupled ultrasound. *Ultrasonics*. 1995. Vol.33. P.11 – 17.
4. **Windels E., Leroy O.** Air – coupled ultrasonic testing of diffusion bonds. *Ultrasonics*. 2002. Vol. 40. P. 171 – 176.
5. **Robertson T. J., Hutchins D. A., Billson D. R.** Surface metrology using reflected ultrasonic signals in air. *Ultrasonics*. 2002. Vol.39. P.476 – 486.
6. **Brassier P., Hosten B., Vulovic F.** High – frequency transducers and correlation method to enhance ultrasonic gas flow metering. *Flow Measurement and Instrumentation*. Vol.12. P.201 – 211.

7. **Magori V., Walker H.** Ultrasonic presence sensors with wide range and high local resolution. IEEE Trans. Ultrason. and Freq. Control. Vol. UFFC – 34. 1987. P.202 – 211.
8. **Dell Isola M., Cannizzo M., Diritti M.** Measurement of high – pressure natural gas flow using ultrasonic flowmeters. Measurement. 1997. Vol.20. No.2. P.75 – 89.
9. **Holden J. L., Peters J. W.** Practical experiences using ultrasonic flowmeters on hogh pressure gas. Flow Meas. Instrum. 1991. Vol.2. P 69 – 73.
10. **Buckley J.** principles and application of air – coupled ultrasonics. Insight. 1998. Vol.40. No.11. P.755 – 759.
11. **Домаркас В. И., Кажис Р.–И. Ю.** Контрольно – измерительные пьезоэлектрические преобразователи. Вильнюс: Минтис. 1975.
12. **Кажис Р.–И.** Ультразвуковые информационно – измерительные системы. Вильнюс: Мокслас.1986.

R. Kažys, A. Vladišauskas, E. Žukauskas

Plačiajuosčiai ultragarsiniai keitikliai matuoti oro aplinkoje

Reziumė

Nagrinėjami plačiajuosčiai ultragarsiniai pjezokeitikliai darbui dujų aplinkoje. Pateikta keitiklio konstrukcija, sumodeliuotos keitiklio perdavimo funkcijos įvertinus suderinimo sluoksnių įtaką. Atlikus eksperimentinį keitiklių tyrimą, nustatytos jų laikinės bei dažninės charakteristikos esant skirtingam sužadininui. Aptarti jų pritaikymo aviacinės paskirties medžiagoms (GLARE, anglies pluoštu sutvirtintoms plastmasinėms) tirti ir dujų srauto greičiui matuoti atvejai.

Pateikta spaudai 2004 09 30